Rate of Silver Nanoparticle Aggregation Based on pH and Capping Agent Length



Eric Coltrain

Senior Comprehensive Project

Allegheny College – Class of 2021

Submitted to the Department of Biochemistry of Allegheny College in partial fulfillment of the requirement for the degree of Bachelor of Science

Committee Members:

Alice Deckert (Research Advisor)

Dr. Tricia Humphreys

Ivelitza Garcia

I hereby recognize and pledge to fulfill my responsibilities as defined in the Honor Code and to maintain the integrity of both myself and the College community as a whole.

Pledge: Eric Coltrain

Table of Contents

Acknowledgments……1

Abstract……2

Background and Significance…….....3

Specific Aims.....7

Experimental Design.....8

Results.....12

References.....16

Acknowledgements:

Dr. Deckert, thank you for your support through my years at Allegheny and everything you have done for me my Senior year.

Mom and Dad, thank you for always supporting me through both the best and the worst of times. No matter what happened I could always count on your support in every aspect of my life.

Nick and Ben, thank you for your insight in working on this composition. Your advice has been invaluable.

Abstract

Silver nanoparticles possess antimicrobial properties that cause them to be frequently used and studied in a medical environment. Aggregation of silver nanoparticles inhibits the antimicrobial effects. In this work the mechanisms of aggregation were studied utilizing Localized Surface Plasmon Resonance. Borohydride and polyethylene glycol were used as capping agents to control aggregation and assist in quantifying the rate. A rate constant of $0.0388 M^{-1}s^{-1}$ was determined for the second order reaction of aggregation of uncapped silver nanoparticles.

Background and Significance

Nanoparticles are increasingly used not only in research, but in industrial and consumer products as well.[1-2] Silver nanoparticles, being the most well studied type of nanoparticles, are known to be cytotoxic to microbial organisms and sea life.[3-4-5-6] However, there are few scientific papers which analyze the specific nature of silver nanoparticle aggregation. Aggregated silver nanoparticles are less cytotoxic than unaggregated silver nanoparticles.[7] Therefore proper understanding of how nanoparticle aggregation occurs is crucial to furthering the usage of nanoparticles.

Silver nanoparticles possess a neutral charge, unlike the positive charge of silver ions and most forms of silver possess. The absence of electrostatic repulsion causes the silver atoms to associate with each other in solution to form nanoparticles. Silver in most forms has a strong cytotoxic effect, however silver nanoparticles provide a unique means for killing pathogens with a high efficacy.[8] The differing charges in ionic silver and silver nanoparticles allows for different localizations within organisms.[9]

Heavy metals are known to be toxic. While lead is more well-known due to its common usage in industrial settings and newsworthy incidents such as the Flint Michigan water crisis, silver is also a heavy metal which has low toxicity to humans but is still extremely toxic to microbial organisms.[9] Due to the lower surface area – volume ratio, aggregated silver nanoparticles are substantially less toxic than unaggregated silver nanoparticles.

Aggregation refers to a number of particles coming together in solution to form a clump. (Figure 1) In this study, the goal is to quantify the rate at which silver nanoparticles aggregate under pH shifts and varying capping agent lengths. Changes in pH are known to have an impact on the aggregation of nanoparticles.[10] Different capping agents are known to have different effects on nanoparticle aggregation, with most preventing aggregation, while some can induce controlled aggregation.[11]

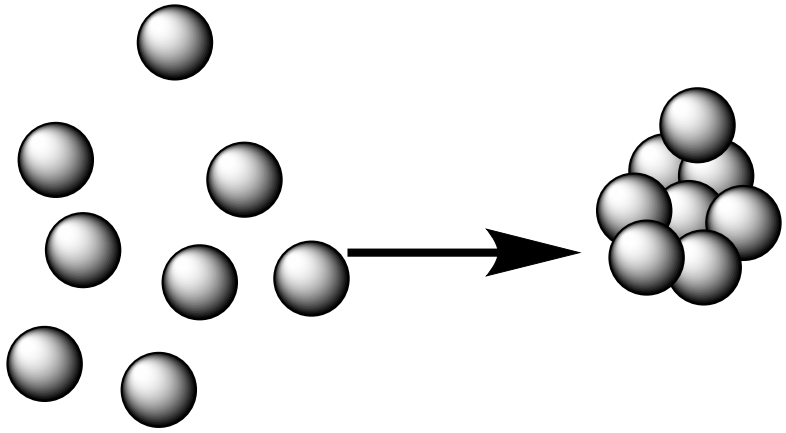


Figure 1: A representation of the aggregation of particles

Capping agents are specific molecules that attach to the surface of nanoparticles and interfere with the direct intermolecular interactions between nanoparticles.[12-13] This often stabilizes the nanoparticles by preventing them from forming aggregates.[14-15] There are 3 major ways in which capping agents can stabilize nanoparticles: Steric stabilization, Electrostatic stabilization, and Electro-steric stabilization.[12] Electro-steric stabilization is a combination of the two other major ways in which capping agents stabilize nanoparticles, as such the focus of this study will be on Steric and Electrostatic stabilization.

Steric stabilization utilizes capping agents with a "head group" attached to the nanoparticle while the "tail group" of the capping agent extends outward from the nanoparticle.[12] With large tail groups surrounding each nanoparticle it is difficult for individual nanoparticles to interact with each other, and consequently prevents aggregation (Figure 2).[12]

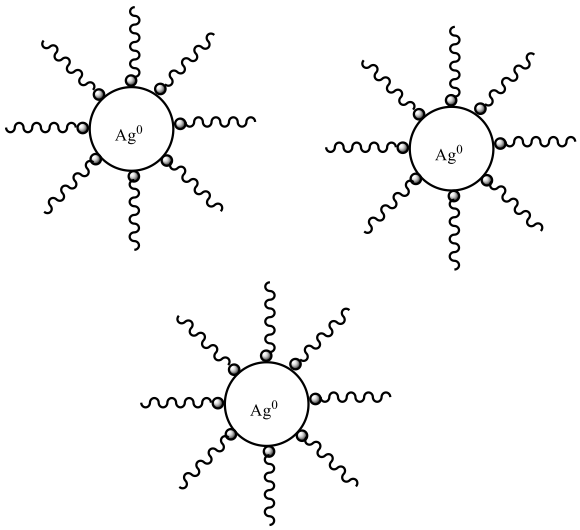


Figure 2: A representation of steric stabilization on silver nanoparticles. The silver nanoparticles are unable to interact with each other due to the large tails separating the nanoparticles.

Electrostatic stabilization utilizes charged capping agents which repel each other while attaching to the nanoparticles. Due to the ability of electrons to freely move within nanoparticles the addition of a charged capping agent creates a dipole along the particle's surface which aids in keeping the charged capping agent attached. (Figure 3) However, the dipole moment created by this interaction is capable of causing an attractive force with smaller nanoparticles.[12]

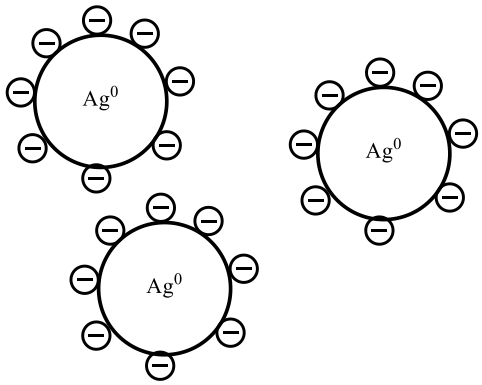


Figure 3: A representation of electrostatic stabilization on silver nanoparticles. The negative charges repel the nanoparticles from interacting with each other.

In order to measure nanoparticle aggregation, a phenomenon known as Localized Surface Plasmon Resonance (LSPR) will be utilized.[16] This phenomenon occurs when light of a specific frequency passes over a nanoparticle of a specific size. This excites the electrons within the nanoparticle, and because these electrons are capable of moving freely they are capable of

oscillating in tandem with the frequency of the light wave.[17] (Figure 4) The frequency at which this phenomenon occurs depends on the size of the nanoparticle, and as such LSPR occurs at a different frequency with aggregated nanoparticles than is does with unaggregated nanoparticles. This causes aggregated nanoparticles to be viewed as a different color than unaggregated nanoparticles. (Figure 5) The oscillation of these electrons causes some of the light to be absorbed and converted into heat, while the rest is scattered off the surface. While it is possible to measure the heat caused by the absorption, this study will utilize the scattered light to quantify nanoparticle aggregation using a spectrometer.

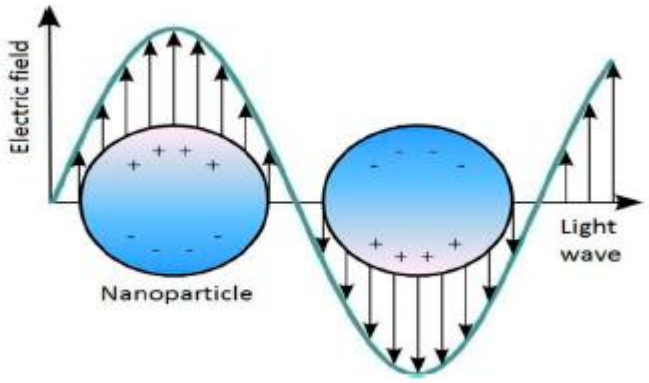


Figure 4: A representation of the interaction of LSPR on the surface of a nanoparticle. Figure duplicated from reference 14.[14]

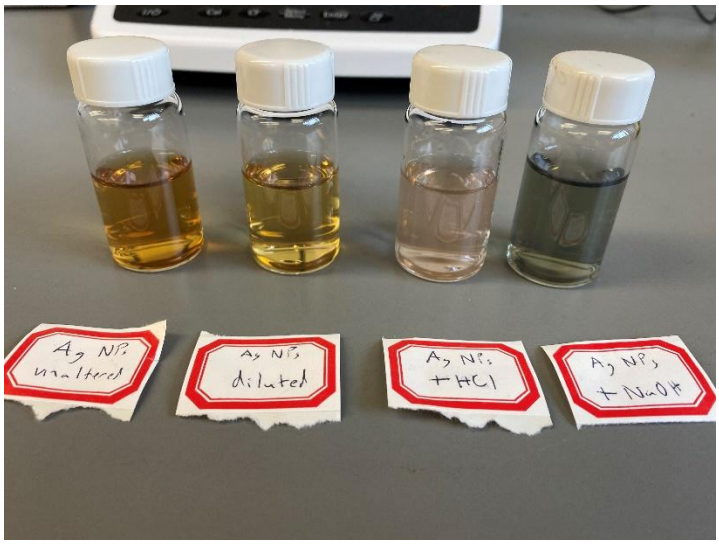


Figure 5: Silver nanoparticles under different conditions with different aggregation levels. The solutions are from right to left: Unaltered silver nanoparticles, Silver nanoparticles diluted with distilled water, Silver nanoparticles with 0.1M HCl, Silver nanoparticles with 0.1M NaOH. Unaltered nanoparticles appear yellow, while low pH nanoparticles appear pink and high pH nanoparticles appear blueish-gray.

Specific Aims

In order to obtain a fuller understanding of the mechanisms of nanoparticle aggregation several variables must be measured. The first aim is to measure the effects of pH on aggregation rate, as pH is already known to have a positive effect on aggregation.[10] Using pH to force aggregation, further measurements can be made on other variables, such as capping agent length, which effect aggregation. Both increases and decreases in pH will be used and compared to determine at which pH experiments to achieve any future aims would be most optimally performed at.

The second aim is to compare the effects of steric and electrostatic capping agents on stability of nanoparticles. The two types of nanoparticle stabilization will be compared by using an equal shift in pH and comparing the rate at which both aggregate. A large, steric capping agent in thiolated polyethylene glycol and a small, electrostatic capping agent in borohydride will be used to compare these effects. (Figure 6)

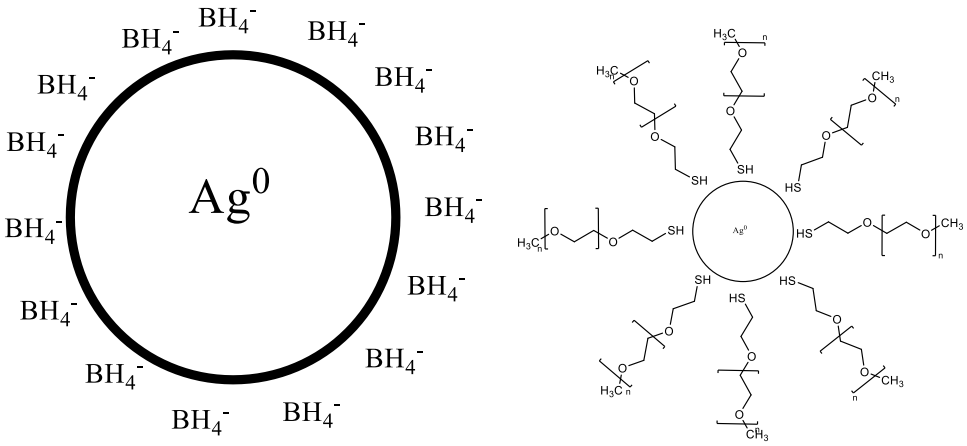


Figure 6: A representation of the capping of silver nanoparticles with borohydride (left) and thiolated polyethylene glycol (right)

The third aim is to compart the effects of the length of steric capping agents on the stability of nanoparticles. Thiolated polyethylene glycol's effects on aggregation will be measured with a sample of 800 mn thiolated polyethylene glycol and a sample of 6000 mn thiolated polyethylene glycol. Mn represents the average molecular weight of the thiolated polyethylene glycol within the sample.

Experimental Design

The first step is the production of silver nanoparticles. An 800mL batch of 2.5×10^{-4}M silver nanoparticles was produced using 0.001M Silver Nitrate ($AgNO_3$) and .0020M Sodium Borohydride ($NaBH_4$).[18] The chemical reaction for $AgNO_3$ and $NaBH_4$:

$$AgNO_3 + NaBH_4 \rightarrow Ag + \frac{1}{2}H_2 + \frac{1}{2}B_2H_6 + NaNO_3$$

These solutions were mixed 10 mL $AgNO_3$ and 30 mL $NaBH_4$ at a time and added to a batch until 800mL was produced. The resulting nanoparticles were a pale yellow color with a wavelength peak at 432nm. (Figure 7) This suggests the nanoparticles are approximately 9.5 ± 3.2nm large and spherical in shape.[19-20] While there are many different ways to prepare silver nanoparticles, the method with $NaBH_4$ was chosen because it allows for alteration of the capping agent. An alternate method using hydrazine (N_2H_4) was also tested,[21] however that method provided inconsistent results.

UV-VIS spectroscopy will be used to measure the aggregation of silver nanoparticles. The fraction of nanoparticles aggregated in a specific experiment can be calculated by comparing the initial absorbance at a wavelength determined through experimentation of unaggregated nanoparticles to the final absorbance of unaggregated nanoparticles. However, this method cannot be used to measure the rate of absorbance, as to effectively measure the absorbance of the unaggregated nanoparticles one must measure the area under the curve for the specific peak. As a time-lapse using a UV-Vis Spectrometer can only be performed on 1-2 wavelengths at a time the area under the curve cannot be measured with the instrumentation at Allegheny College's disposal (Figure 7). As such, a different method to determine the ratio of aggregated to unaggregated nanoparticles must be performed.

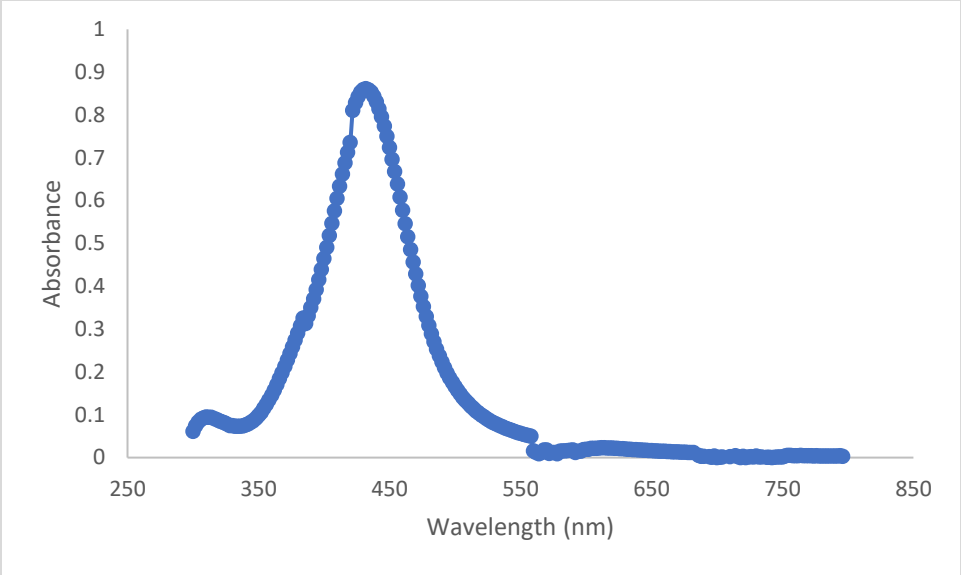


Figure 7: Unaggregated silver nanoparticles. A peak was formed at 432nm, however the range over which unaggregated nanoparticles resonate ranges from 350-500.

By dividing the absorbance of the aggregated peak of silver nanoparticles by the original peak the ratio of aggregated silver nanoparticles can be calculated.[22] The peak of aggregated silver nanoparticles was determined to be 587nm. This peak was determined by increasing the pH of a solution to the point where almost all nanoparticles aggregated. Using this method, the ratio of aggregated nanoparticles to unaggregated nanoparticles can be determined.

To measure the rate data will first be collected to determine how much the nanoparticles aggregate under specific conditions, if at all, and whether the rate at which they aggregate is easily measurable. Nanoparticle aggregation normally occurs rather quickly, usually requiring less than 5 minutes to completely aggregate.[23] In order to determine this an initial measurement will be run immediately upon a system being put under specific conditions, and then measured again after 15 minutes. The measurements will be compared to both a control and to each other. If there is no significant difference between the control and the altered system then the conclusion that aggregation did not occur. If there is a difference between the control and the altered system's measurements, however the initial measurement and the delayed measurement are not statistically different, then the conclusion can be drawn that the nanoparticles fully aggregate to quicky accurate measurement with simple methods. If the delayed measurement is significantly different from both the control and initial measurement then the conclusion can be drawn that aggregation occurred at a measurable rate.

In order to first determine the pH at which all further experiments should be run, the pH was increased with 0.1M NaOH of various volumes, (Figure 8) and decreased with 0.1M HCl (Figure 9). For each shift in pH the UV-Vis spectrum was measured once initially and a second time after waiting 15 minutes. For each measurement the absorbance at 587nm was divided by the absorbance at 432nm to determine the ratio of aggregated to unaggregated nanoparticles. The data collected suggests that aggregation occurs at both significantly increased pH and significantly decreased pH, however at increased pH the rate of aggregation is too fast to be reliably quantified using a UV-Vis spectrometer. While other methods such as stopped-flow could be used to measure the rate of aggregation of these high pH samples, due to time constraints the focus will be on low pH samples.

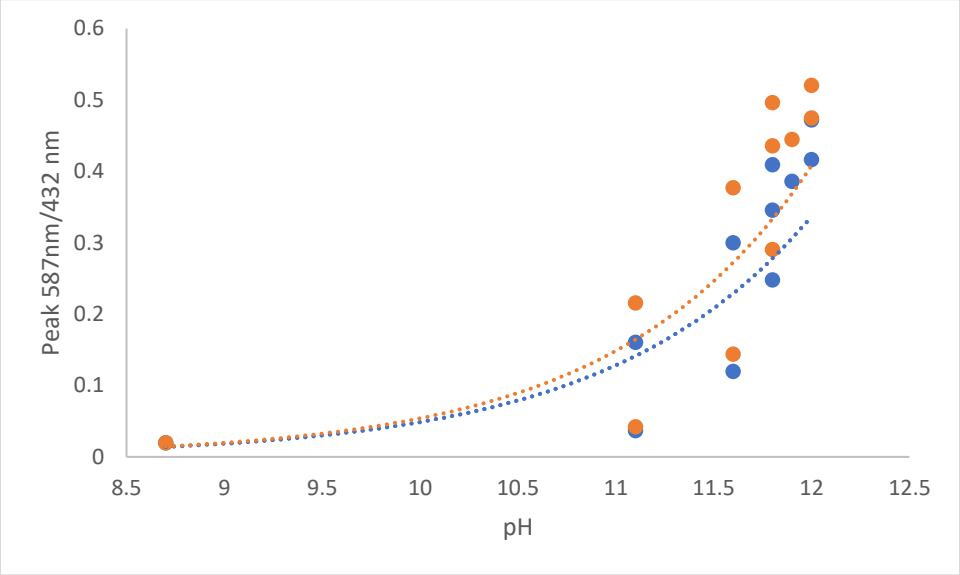


Figure 8: Plot of nanoparticle aggregation at increased pH. The blue series determined the aggregation after 30 seconds. The orange series determined aggregation after 15 minutes. An F-test was performed to find no statistical difference between these two samples. The furthermost left sample represents nanoparticles with unaltered pH

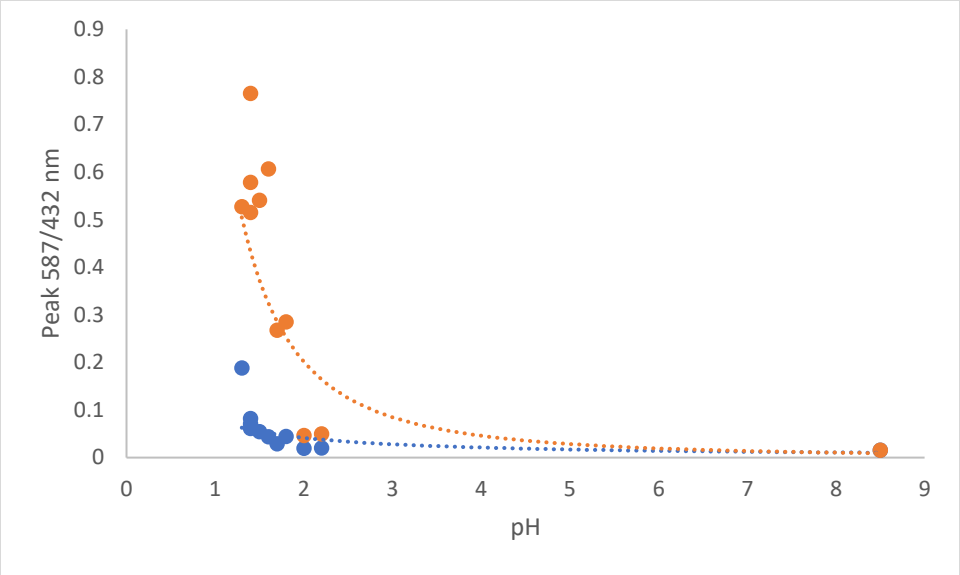


Figure 9: Plot of nanoparticle aggregation at decreased pH. The blue series determined the aggregation after 30 seconds. The orange series determined aggregation after 15 minutes. An F-test reveals these lines to be statistically different. The furthermost right sample represents nanoparticles with unaltered pH.

All further experiments will be conducted at pH 1.9 or less. Using the time-lapse function on the UV-Vis spectrometer will cause a data point to be collected every second, so by using this function at the desired frequencies of 432 and 587 nm the rate can be graphed. Due to the constraints of the instrument being used only one can be taken at a time, so multiple samples must be prepared for each measurement.

Samples of nanoparticles capped with varying concentrations of thiolated polyethylene glycol were prepared. 0.010g of 800mn thiolated polyethylene glycol was added to 10mL of distilled water and dissolved. Quantities of thiolated polyethylene glycol solution ranging from 0.25mL to 1.0mL were added to 10mL of silver nanoparticle solution. Sulfur is less electronegative than boron, and as such the thiolated polyethylene glycol will gradually replace the borohydride on the surface of the nanoparticles. The nanoparticle solutions were left overnight to allow this to occur.

Results

For borohydride capped nanoparticles the pH was reduced to 1.8 and measured over the course of 960 seconds (15 minutes). Data was collected at both 432 nm and 587 nm. By dividing the peak at 587 nm by the peak at 432 nm the ratio of aggregated to unaggregated nanoparticles was determined at each point in time. (Figure 10) The trendline was found to be a power equation which means that this reaction is a second order reaction with respect to the reactant.[24]

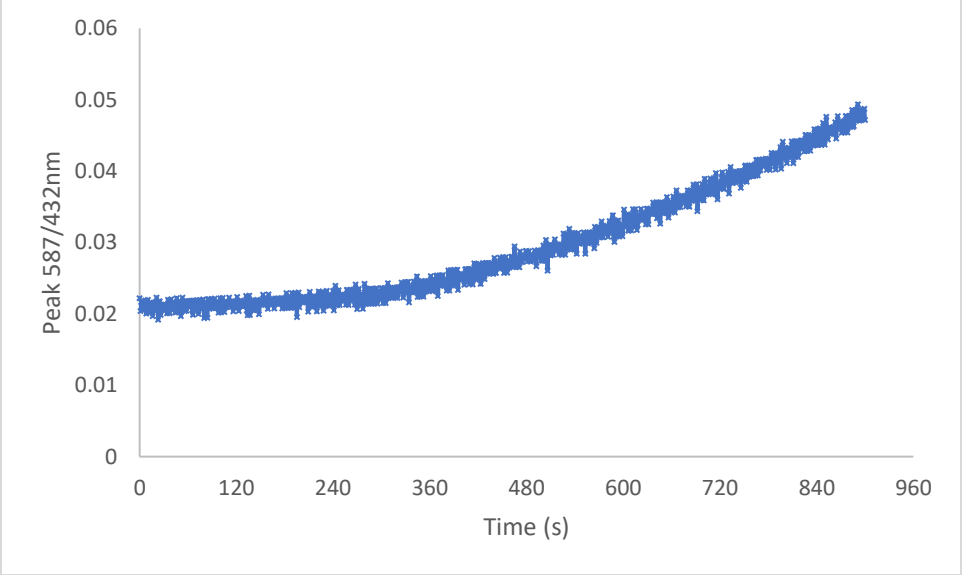


Figure 10: The ratio of aggregated nanoparticles to unaggregated nanoparticles over time for borohydride capped nanoparticles at pH 1.8. A trendline with the equation y = 4E-08x² - 5E-06x + 0.0212 was determined.

The rate of second order reactions can be determined using the equation:

$$R = k[A]^2$$

Where R is the rate, k is the rate constant, and [A] is the concentration of reactants, or in this case unaggregated nanoparticles. In order to determine the rate constant, all that needs to be done is to graph the 1/(peak 587/432) vs. time and k is equal to the slope. (Figure 11) As the figure clearly demonstrates there is a shift between 300 and 360 seconds where the slope changes. For the first 300 seconds the slope is -0.0115. (Figure 12) After the first 360 seconds the slope is -0.0388. In this case, the slope is equal to the negative k value with respect to nanoparticle aggregation. This makes the initial rate equation of borohydride capped nanoparticles at pH 1.8

$R = 0.0115[A]^2$ and the secondary rate equation of borohydride capped nanoparticles at pH 1.8 $R = 0.0388[A]^2$.

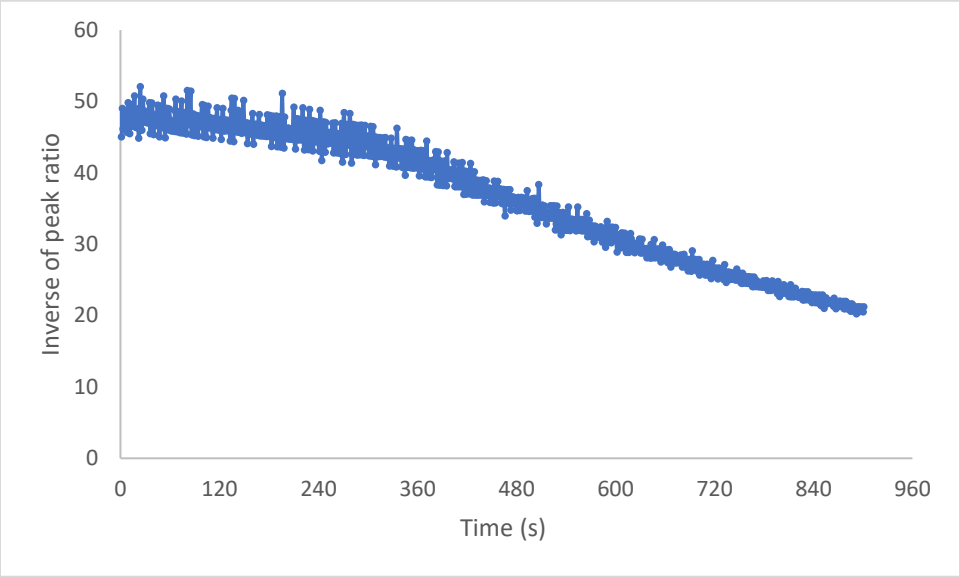


Figure 11: The inverse of the ratio of aggregated nanoparticles to unaggregated nanoparticles over time. The rate appears to change at roughly 300 seconds from one linear slope to a different linear slope

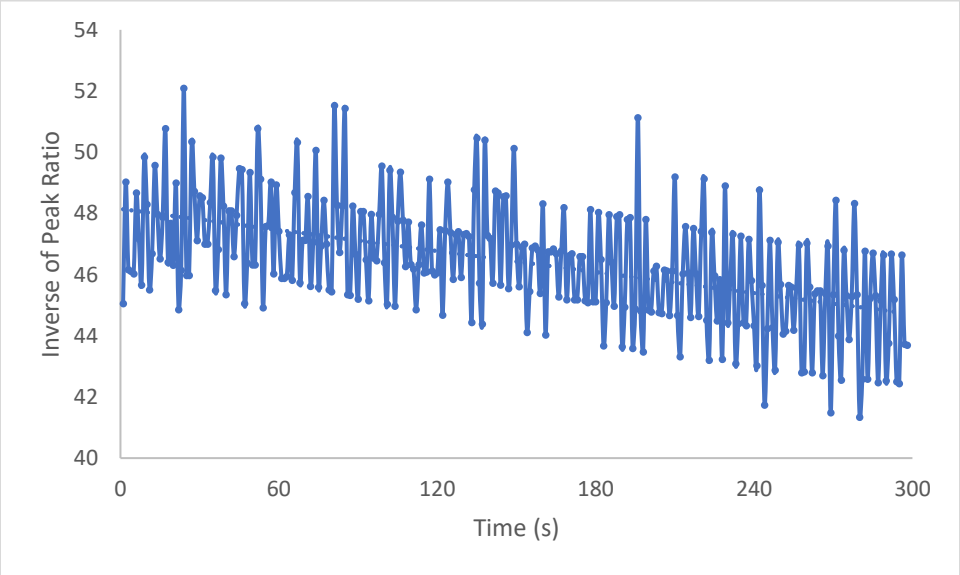


Figure 12: The first 300 seconds of figure 11. This possesses a linear line of best fit with the equation y = -0.0115x + 48.146

Slope is -0.0115

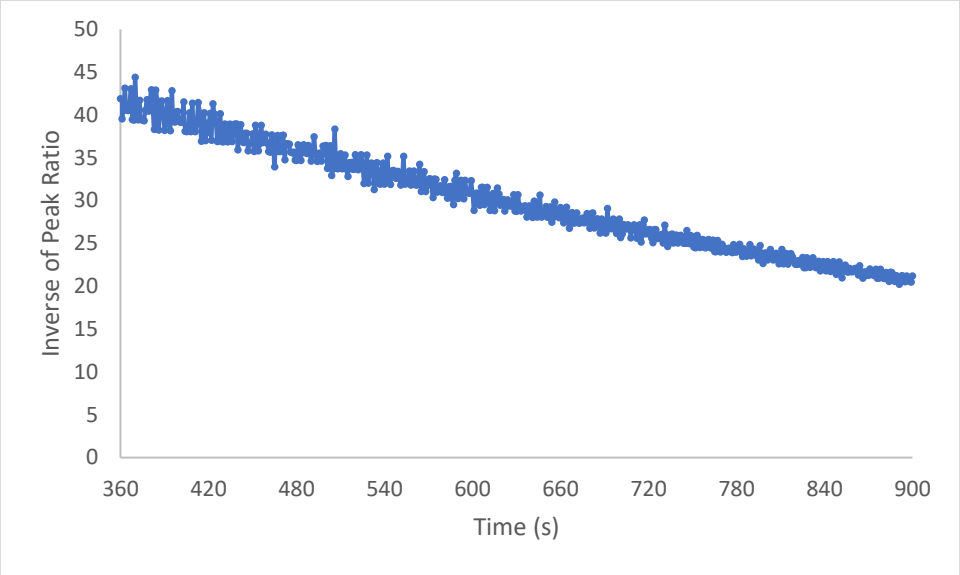


Figure 13: The final 440 seconds of Figure 11. This possesses a linear line of best fit with the equation y = -0.0388x + 54.532 Slope is -0.0388

The shift of the rate of aggregation after a few minutes likely occurs due to an initial interaction occurring between the hydronium ions (H_3O^+) found in low pH solutions and the borohydride capped on the surface of the nanoparticles. Due to the need for the capping agent to be removed from the surface of the nanoparticles in order for them to aggregate the actual aggregation cannot occur until the borohydride has sufficiently reacted with the H_3O^+. As such the initial determined rate is likely aggregation occurring while this reaction is still occurring. The secondary rate likely appears once the capping agent is fully removed from the surface of the nanoparticles and the nanoparticles are able to aggregate freely. The secondary rate reaction of $R = 0.0388[A]^2$ is likely the rate of aggregation of nanoparticles that are not stabilized by a capping agent.

Due to time constraints the rate of aggregation could not be measured over a large pH range, however due to the increase in the ratio of aggregated nanoparticles compared to unaggregated nanoparticles over larger pH shifts (Figure 9) it is likely that as the shift in pH increases the initial rate of aggregation also increases, however the secondary rate of reaction would likely remain the same.

When attempting to repeat the experiment with thiolated polyethylene glycol capped nanoparticles the nanoparticles failed to aggregate. Additional attempts to force nanoparticle

aggregation with lower pH, higher pH, and the addition of sodium chloride all failed to cause aggregation. While electrostatic based capping agents can be separated from the surface of nanoparticles by the addition of charged ions to the solution by way of pH shifts or the addition of salts, steric based capping agents are resistant to this effect due to the fact that they do not possess a charge.

There are other ways to force nanoparticle aggregation, such as altering temperature, washing, or sonication,[24] however due to time constraints this study was unable to continue with these methods. Alternatively adding specific analytes beyond salts, such as arsenite, are also known to induce aggregation.[25] Unfortunately, these time constraints prevented the completion of specific aims 2 and 3. With additional time and resources both specific aims 2 and 3 could be met, as well as a more complete fulfillment of specific aim 1.

References

(1) Wang, H.; Burgess, R. M.; Cantwell, M. G.; Portis, L. M.; Perron, M. M.; Wu, F.; Ho, K. T. Stability and Aggregation of Silver and Titanium Dioxide Nanoparticles in Seawater: Role of Salinity and Dissolved Organic Carbon. *Environ. Toxicol. Chem.* **2014**, *33* (5), 1023–1029. https://doi.org/10.1002/etc.2529.

(2) Afshinnia, K.; Gibson, I.; Merrifield, R.; Baalousha, M. The Concentration-Dependent Aggregation of Ag NPs Induced by Cystine. *Sci. Total Environ.* **2016**, *557–558*, 395–403. https://doi.org/10.1016/j.scitotenv.2016.02.212.

(3) Jeremiah, S. S.; Miyakawa, K.; Morita, T.; Yamaoka, Y.; Ryo, A. Potent Antiviral Effect of Silver Nanoparticles on SARS-CoV-2. *Biochem. Biophys. Res. Commun.* **2020**, *533* (1), 195–200. https://doi.org/10.1016/j.bbrc.2020.09.018.

(4) Mylona, Z.; Panteris, E.; Kevrekidis, T.; Malea, P. Silver Nanoparticle Toxicity Effect on the Seagrass Halophila Stipulacea. *Ecotoxicol. Environ. Saf.* **2020**, *189* (September 2019), 109925. https://doi.org/10.1016/j.ecoenv.2019.109925.

(5) Mahmoud, U. M.; Mekkawy, I. A. A.; Naguib, M.; Sayed, A. E. D. H. Silver Nanoparticle–Induced Nephrotoxicity in Clarias Gariepinus: Physio-Histological Biomarkers. *Fish Physiol. Biochem.* **2019**, *45* (6), 1895–1905. https://doi.org/10.1007/s10695-019-00686-7.

(6) Huang, Z.; Zeng, Z.; Song, Z.; Chen, A.; Zeng, G.; Xiao, R.; He, K.; Yuan, L.; Li, H.; Chen, G. Antimicrobial Efficacy and Mechanisms of Silver Nanoparticles against Phanerochaete Chrysosporium in the Presence of Common Electrolytes and Humic Acid. *J. Hazard. Mater.* **2020**, *383* (September 2019), 121153. https://doi.org/10.1016/j.jhazmat.2019.121153.

(7) Bélteky, P.; Rónavári, A.; Igaz, N.; Szerencsés, B.; Tóth, I. Y.; Pfeiffer, I.; Kiricsi, M.; Kónya, Z. Silver Nanoparticles: Aggregation Behavior in Biorelevant Conditions and Its Impact on Biological Activity. *Int. J. Nanomedicine* **2019**, *14*, 667–687. https://doi.org/10.2147/IJN.S185965.

(8) Kedziora, A. Silver Ions Vs Silver Nanoparticles as Antibacterial Factor. *EC Microbiol.* **2017**, *5*, 125–127.

(9) Lacave, J. M.; Vicario-Parés, U.; Bilbao, E.; Gilliland, D.; Mura, F.; Dini, L.; Cajaraville, M. P.; Orbea, A. Waterborne Exposure of Adult Zebrafish to Silver Nanoparticles and to Ionic Silver Results in Differential Silver Accumulation and Effects at Cellular and Molecular Levels. *Sci. Total Environ.* **2018**, *642*, 1209–1220. https://doi.org/10.1016/j.scitotenv.2018.06.128.

(10) Keller, A. A.; Wang, H.; Zhou, D.; Lenihan, H. S.; Cherr, G.; Cardinale, B. J.; Miller, R.; Zhaoxia, J. I. Stability and Aggregation of Metal Oxide Nanoparticles in Natural Aqueous Matrices. *Environ. Sci. Technol.* **2010**, *44* (6), 1962–1967. https://doi.org/10.1021/es902987d.

(11) Roca, M.; Haes, A. J. Probing Cells with Noble Metal Nanoparticle Aggregates. *Nanomedicine* **2008**, *3* (4), 555–565. https://doi.org/10.2217/17435889.3.4.555.

(12) Canyon Hydro; Summary, E.; Of, F.; Potential, T. H. E.; Ferreres, X. R.; Font, A. R.; Ibrahim, A.; Maximilien, N.; Lumbroso, D.; Hurford, A.; Winpenny, J.; Wade, S.; Sataloff, R. T.; Johns, M. M.; Kost, K. M.; State-of-the-art, T.; Motivation, T.; Norsuzila Ya'acob1, Mardina Abdullah1, 2 and Mahamod Ismail1, 2; Medina, M.; Talarico, T. L.; Casas, I. A.; Chung, T. C.; Dobrogosz, W. J.; Axelsson, L.; Lindgren, S. E.; Dobrogosz, W. J.; Kerkeni, L.; Ruano, P.; Delgado, L. L.; Picco, S.; Villegas, L.; Tonelli, F.; Merlo, M.; Rigau, J.; Diaz, D.; Masuelli, M. We Are IntechOpen , the World ' s Leading Publisher of Open Access Books Built by Scientists , for Scientists TOP 1 %. *Intech* **2013**, *32* (July), 137–144.

(13) Nowsath Rifaya, M.; Theivasanthi, T.; Alagar, M. Chemical Capping Synthesis of Nickel Oxide Nanoparticles and Their Characterizations Studies. *Nanosci. Nanotechnol.* **2012**, *2* (5), 134–138. https://doi.org/10.5923/j.nn.20120205.01.

(14) Amaliyah, S.; Pangesti, D. P.; Masruri, M.; Sabarudin, A.; Sumitro, S. B. Green Synthesis and Characterization of Copper Nanoparticles Using Piper Retrofractum Vahl Extract as Bioreductor and Capping Agent. *Heliyon* **2020**, *6* (8), e04636. https://doi.org/10.1016/j.heliyon.2020.e04636.

(15) Tanner, E. E. L.; Batchelor-McAuley, C.; Compton, R. G. Nanoparticle Capping Agent Controlled Electron-Transfer Dynamics in Ionic Liquids. *Chem. - A Eur. J.* **2016**, *22* (17), 5976–5981. https://doi.org/10.1002/chem.201505117.

(16) Song, X.; Liu, J.; Shi, F.; Fan, C.; Ran, S.; Zhang, H.; Zou, Z. Facile Fabrication of KmCsnWO3 with Greatly Improved Near-Infrared Shielding Efficiency Based on W5+-Induced Small Polaron and Local Surface Plasmon Resonance (LSPR) Modulation. *Sol. Energy Mater. Sol. Cells* **2020**, *218* (September), 110769. https://doi.org/10.1016/j.solmat.2020.110769.

(17) Unser, S.; Bruzas, I.; He, J.; Sagle, L. Localized Surface Plasmon Resonance Biosensing: Current Challenges and Approaches. *Sensors (Switzerland)* **2015**, *15* (7), 15684–15716. https://doi.org/10.3390/s150715684.

(18) Solomon, S. D.; Bahadory, M.; Jeyarajasingam, A. V.; Rutkowsky, S. A.; Boritz, C.; Mulfinger, L. Synthesis and Study of Silver Nanoparticles. *J. Chem. Educ.* **2007**, *84* (2), 322–325. https://doi.org/10.1021/ed084p322.

(19) Huang, T.; Xu, X. H. N. Synthesis and Characterization of Tunable Rainbow Colored Colloidal Silver Nanoparticles Using Single-Nanoparticle Plasmonic Microscopy and Spectroscopy. *J. Mater. Chem.* **2010**, *20* (44), 9867–9876. https://doi.org/10.1039/c0jm01990a.

(20) González, A. L.; Noguez, C.; Beránek, J.; Barnard, A. S. Size, Shape, Stability, and Color of Plasmonic Silver Nanoparticles. *J. Phys. Chem. C* **2014**, *118* (17), 9128–9136. https://doi.org/10.1021/jp5018168.

(21) Nickel, U.; Castell, A. Z.; Pöppl, K.; Schneider, S. Silver Colloid Produced by Reduction with Hydrazine as Support for Highly Sensitive Surface-Enhanced Raman Spectroscopy. *Langmuir* **2000**, *16* (23), 9087–9091. https://doi.org/10.1021/la000536y.

(22) Wei, H.; Chen, C.; Han, B.; Wang, E. Enzyme Colorimetric Assay Using Unmodified Silver Nanoparticles. *Anal. Chem.* **2008**, *80* (18), 7051–7055. https://doi.org/10.1021/ac801144t.

(23) Trisaranakul, W.; Chompoosor, A.; Maneeprakorn, W.; Nacapricha, D.; Choengchan, N.; Teerasong, S. A Simple and Rapid Method Based on Anti-Aggregation of Silver Nanoparticles for Detection of Poly(Diallyldimethylammonium Chloride) in Tap Water. *Anal. Sci.* **2016**, *32* (7), 769–774. https://doi.org/10.2116/analsci.32.769.

(24) Mansfield, E. D. H.; Filippov, S. K.; de la Rosa, V. R.; Cook, M. T.; Grillo, I.; Hoogenboom, R.; Williams, A. C.; Khutoryanskiy, V. V. Understanding the Temperature Induced Aggregation of Silica Nanoparticles Decorated with Temperature-Responsive Polymers: Can a Small Step in the Chemical Structure Make a Giant Leap for a Phase Transition? *J. Colloid Interface Sci.* **2021**, *590* (January), 249–259. https://doi.org/10.1016/j.jcis.2021.01.044.

(25) Xue, Q.; Niu, X.; Liu, P.; Wang, M.; Peng, Y.; Peng, H.; Li, X. Analyte-Triggered Citrate-Stabilized Au Nanoparticle Aggregation with Accelerated Peroxidase-Mimicking Activity for Catalysis-Based Colorimetric Sensing of Arsenite. *Sensors Actuators, B Chem.* **2021**, *334* (January). https://doi.org/10.1016/j.snb.2021.129650.